Atmos. Meas. Tech., 8, 2279–2289, 2015
www.atmos-meas-tech.net/8/2279/2015/
doi:10.5194/amt-8-2279-2015

Atmospheric Measurement Techniques
Open Access

Comparison of operational satellite SO_2 products with ground-based observations in northern Finland during the Icelandic Holuhraun fissure eruption

I. Ialongo[1], J. Hakkarainen[1], R. Kivi[2], P. Anttila[3], N. A. Krotkov[4], K. Yang[5], C. Li[4,6], S. Tukiainen[1], S. Hassinen[1], and J. Tamminen[1]

[1]Earth Observation Unit, Finnish Meteorological Institute, Helsinki, Finland
[2]Arctic Research Center, Finnish Meteorological Institute, Sodankylä, Finland
[3]Atmospheric Composition Unit, Finnish Meteorological Institute, Helsinki, Finland
[4]Atmospheric Chemistry and Dynamics Laboratory, NASA Goddard Space Flight Center, Greenbelt, Maryland, USA
[5]Department of Atmospheric and Oceanic Science, University of Maryland College Park, College Park, Maryland, USA
[6]Earth System Science Interdisciplinary Center, University of Maryland, College Park, Maryland, USA

Correspondence to: I. Ialongo (iolanda.ialongo@fmi.fi)

Received: 5 December 2014 – Published in Atmos. Meas. Tech. Discuss.: 16 January 2015
Revised: 4 May 2015 – Accepted: 13 May 2015 – Published: 3 June 2015

Abstract. This paper shows the results of the comparison of satellite SO_2 observations from OMI (Ozone Monitoring Instrument) and OMPS (Ozone Mapping Profiler Suite) with ground-based measurements during the Icelandic Holuhraun fissure eruption in September 2014. The volcanic plume reached Finland on several days during the month of September. The SO_2 total columns from the Brewer direct sun (DS) measurements in Sodankylä (67.42° N, 26.59° E), northern Finland, are compared to the satellite data.

The operational satellite SO_2 products are evaluated for high latitude conditions (e.g. large solar zenith angle, SZA). The results show that the best agreement can be found for lowest SZAs, close-to-nadir satellite pixels, cloud fraction below 0.3 and small distance between the station and the centre of the pixel. Under good retrieval conditions, the difference between satellite data and Brewer measurements remains mostly below the uncertainty on the satellite SO_2 retrievals (up to about 2 DU at high latitudes).

The satellite products assuming a priori profile with SO_2 predominantly in the planetary boundary layer give total column values with the best agreement with the ground-based data.

The analysis of the SO_2 surface concentrations at four air quality stations in northern Finland shows that the volcanic plume coming from Iceland was located very close to the surface. This is connected to the fact that this was a fissure eruption and most of the SO_2 was emitted into the troposphere. This is an exceptional case because the SO_2 volcanic emissions directly affect the air quality levels at surface in an otherwise pristine environment like northern Finland. The time evolution of the SO_2 concentrations peaks during the same days when large SO_2 total column values are measured by the Brewer in Sodankylä and enhanced SO_2 signal is visible over northern Finland from the satellite maps. Thus, the satellite retrievals were able to detect the spatiotemporal evolution of the volcanic plume as compared to the surface observations.

Furthermore, direct-broadcast SO_2 satellite data (from both OMI and OMPS instruments) are compared for the first time against ground-based observations.

1 Introduction

Atmospheric sulfur dioxide (SO_2) has significant impacts on the environment and climate. SO_2 is oxidised to form sulphate aerosols, which in turn participate to the stratospheric ozone destruction (Hofmann and Solomon, 1989) and cause Earth surface cooling (Charlson et al., 1990), by reflecting the incoming solar radiation. SO_2 is generated by

natural sources (e.g. degassing and eruptions of volcanoes, sea spray) and anthropogenic sources (e.g. combustion processes). SO_2 is toxic when present in high concentrations at the surface and negatively affects human health.

SO_2 has been measured from space since the 1982 eruption of El Chichón (Krueger, 1983; Krueger et al., 2008). This was the first time when SO_2 from satellite measurements could be determined from UV-VIS sensors. Those measurements were carried out by Total Ozone Mapping Spectrometer (TOMS), which had a limited SO_2 detection sensitivity, since the discrete measurement wavelengths were designed for total ozone retrieval (Gurevich and Krueger, 1997). Since then, next-generation space-borne spectrometers like GOME (Global Ozone Monitoring Experiment) and GOME-2, SCIAMACHY (SCanning Imaging Absorption spectroMeter for Atmospheric CHartographY) and OMI (Ozone Monitoring Instrument) have shown greatly improved SO_2 detection sensitivity.

Currently, SO_2 from volcanic eruptions and degassing are routinely monitored using satellite data. For example, satellite measurements of volcanic SO_2 emissions can provide critical information for aviation hazard mitigation (Carn et al., 2008; Brenot et al., 2014). SO_2 has low background, making the volcanic SO_2 plumes clearly distinguishable even at long distance from the source. For example, services like SACS (Support to Aviation Control Service, http://sacs.aeronomie.be) use SO_2 as an indicator for volcanic activity and send email notifications when instrument specific SO_2 thresholds are exceeded (Brenot et al., 2014). Quality and timeliness of satellite data products are essential for these kinds of services. Near real-time satellite products – typically available 3 h after the satellite overpass – are generally used for this purpose. Faster processing can be achieved if the so-called direct-broadcast (DB) data are used. This is possible for example for NASA's Terra, Aqua and Aura satellites as well as the recently launched Suomi National Polar Partnership spacecraft, which hosts the Ozone Mapping Profiler Suite (OMPS). The direct-broadcast concept is based on measuring and simultaneously sending the observations down to Earth for processing. The time needed for SO_2 processing is less than 15 min. However, this option is only available for specific locations on the Earth. Direct-broadcast data are received, for example, in Sodankylä (Finland), and SO_2 maps over central and northern Europe are available from SAMPO (Satellite measurements from Polar orbit, http://sampo.fmi.fi) service, which is built on the heritage of OMI Very Fast Delivery (Leppelmeier et al., 2006; Hassinen et al., 2008). This location is especially suitable for receiving DB data since several overpasses are available during 1 day.

The opportunities to validate volcanic SO_2 satellite products are rare, because only occasionally the volcanic plumes drift over a ground-based station where SO_2 measurements are performed. The first successful attempt to validate volcanic OMI SO_2 took place in 2008 after the Okmok volcanic eruption (Spinei et al., 2010). This was followed by an "opportunistic" validation study of Sarychev Peak volcanic eruption cloud, using a mobile ground-based instrument (Carn and Lopez, 2011). The conclusion of the latter study was that stationary ground-based measurements would provide better and more easily interpretable validation data. However, both studies show good agreement between ground-based and OMI SO_2 data. In these studies, about 3–5 OMI pixels were compared against ground-based observations.

GOME-2 SO_2 total columns have also been used for monitoring volcanic eruption (Rix et al., 2009) and validated, for example, during the eruption of the Eyjafjallajökull volcano (Iceland) in April and May 2010 using Brewer measurements (Rix et al., 2012). GOME-2 data agreed very well with the Brewer observations at Hohenpeissenberg (Germany), whereas the Brewer instrument at Valentia (Ireland) showed up to 50 % higher SO_2 columns. Part of this difference was due to the fact that the Brewer data were available as daily averages while the GOME-2 measurements represent a snapshot at the time of the overpass. Furthermore, differences can be caused by uncertainties in both satellite and Brewer observations.

In this paper, both OMI and OMPS operational products are used to monitor the spatiotemporal evolution of the volcanic SO_2 cloud generated during the Holuhraun (Iceland) fissure eruption in September 2014. Since the SO_2 plume reached northern Finland, this episode gives the opportunity to compare SO_2 satellite data to the Brewer SO_2 total columns available at Sodankylä ground-based station. Because the satellite retrieval strongly depends on the air mass factor (AMF, the ratio between slant and vertical column density) and on the a priori SO_2 profile, the effects of these parameters on the retrieval are also discussed. Furthermore, the implications of such volcanic eruption on air quality in northern Finland are investigated, combining the time evolution of satellite observations and SO_2 concentrations at surface level. Section 2 describes the data set used in the comparison. The comparison results are presented and discussed in Sect. 3. The main findings of this work are summarised in Sect. 4.

2 Data set

2.1 Satellite SO_2 products

In this study SO_2 total columns from OMI and OMPS satellite instruments are used to monitor the volcanic emissions during the Holuhraun fissure eruption in September 2014. OMI is an UV-VIS spectrometer launched on-board EOS-Aura spacecraft in 2004 (Levelt et al., 2006). The nominal pixel size of OMI is 13 km × 24 km at nadir and 28 km × 150 km at the swath ends. The OMI swath contains 60 cross-track pixels. The current local Equator crossing time is about 13:45. OMI covers the spectral range from 270

to 500 nm with a resolution of about 0.5 nm. The global coverage is achieved in 2 days. Since 2007 the so-called row-anomaly (see http://www.knmi.nl/omi/research/product/rowanomaly-background.php) has reduced the amount of valid pixels for volcanic clouds monitoring. Despite this anomaly, OMI data have been used in numerous studies for monitoring volcanic eruptions and anthropogenic pollution (e.g. Fioletov et al., 2011, 2013; McLinden et al., 2012). In this work, the OMI data corresponding to pixel number from 23 to 56 are not taken into account.

OMPS is an UV spectrometer flying on-board Suomi National Polar-orbiting Partnership spacecraft since 2011 (Flynn et al., 2006), with local Equator crossing time at 13:30. OMPS is a suite of three instruments: a nadir mapper, a nadir profiler and a limb profiler. In this paper the acronym OMPS refers to the nadir mapper instrument only. OMPS measures backscattered UV radiance spectra in the 300–380 nm wavelength range (resolution of 1 nm) with daily global coverage. OMPS is built on a TOMS heritage and its pixel size (50 km × 50 km at nadir and 190 km × 50 km at the edge of the swath) is bigger than OMI, but it is still suitable for anthropogenic SO_2 monitoring, as shown by Yang et al. (2013). The OMPS swath contains 36 cross-track pixels. Recently, Carn et al. (2015) reported the first volcanic SO_2 measurements using OMPS data.

In order to obtain the total SO_2 columns from OMI and OMPS measurements, the same retrieval techniques are applied to both instruments and four different SO_2 total column estimates are provided, based on different assumptions of the SO_2 vertical profile. The assumed SO_2 profile shape is represented by its centre of mass altitude (CMA), defining the vertical region where SO_2 is predominantly distributed. The products are (1) planetary boundary layer (PBL) SO_2 column, corresponding to CMA of 0.9 km, (2) lower tropospheric (TRL) SO_2 column, corresponding to CMA of 2.5 km, (4) upper tropospheric and stratospheric (STL) SO_2 column, corresponding to CMA of 17 km. The TRL, TRM (mid-troposphere) and STL data products are processed using the linear fit (LF) algorithm designed for large volcanic SO_2 loads (Yang et al., 2007) and the PBL product is retrieved using the band residual difference (BRD) algorithm (Krotkov et al., 2006, 2008). Both BRD and LF algorithms take the residual after the ozone retrieval (SO_2 assumed zero) as an input. In the current OMI PBL standard product, the BRD algorithm has been replaced with the recently developed principal component analysis (PCA) algorithm (Li et al., 2013). The SO_2 retrieval algorithm information are summarised in Table 1.

In this study, OMI SO_2 standard products (SP, available at http://mirador.gsfc.nasa.gov) and the OMI and OMPS direct-broadcast data products are used. The direct-broadcast data are received through the ground-based antennas located in Sodankylä, northern Finland. OMI and OMPS DB images are available from SAMPO (http://sampo.fmi.fi) website. Note that OMPS operational data are not yet distributed and they are not included in this study. Thus, the OMPS data correspond here to the direct-broadcast data set, while OMI data are available as both standard product and direct-broadcast data sets. The DB algorithm uses the "latitude band average" as residual correction method, while the operational algorithm uses the "sliding median" technique, which requires a complete orbit to perform the correction (see Yang et al., 2007, for details). Because of these different methods and the observed difference of L1B data between DB and routine processing, differences between SO_2 DB and SP products are expected. Assessing the quality of the DB retrievals is also important as they are used for volcanic emission real-time services and aviation hazard mitigation (e.g. SACS).

Table 1. Summary of the SO_2 retrieval algorithms.

Product[a]	CMA[b] (km)	Algorithm	Reference
PBL	0.9	BRD[c]	Krotkov et al. (2006)
		PCA[d]	Li et al. (2013)
TRL	2.5		
TRM	7.5	LF[e]	Yang et al. (2007)
STL	17		

[a] Satellite SO_2 total column optimised for different altitude regions: planetary boundary layer (PBL), lower troposphere (TRL), mid-troposphere (TRM) and lower stratosphere (STL).
[b] Centre of mass altitude (CMA).
[c] Band residual difference (BRD).
[d] Principal component analysis (PCA), available for OMI standard product only.
[e] Linear fit (LF).

The accuracy and precision of the retrieved SO_2 column depend on various factors like CMA, SO_2 column amount, measurement geometry, ozone slant column density, solar zenith angle (SZA) and viewing zenith angle (VZA). For OMI, the SO_2 README file v.1.2.0 (available at http://so2.gsfc.nasa.gov/Documentation/OMSO2Readme_V120_20140926.htm) discusses the error estimates of the standard products. One way to study the error estimates is to study SO_2 retrievals in a pristine, presumably SO_2-free location, like the Equatorial Pacific. A recent study by Li et al. (2013) reports standard deviations (STDs) of about 0.5 and 1 DU for PBL PCA and PBL BRD algorithms, respectively. For TRL, TRM and STL algorithms the STDs are reported in the README file as 0.7, 0.3 and 0.2 DU, respectively.

A similar study can be conducted at high latitudes too. The results of this analysis are shown in Sect. 3.3.

2.2 Ground-based measurements

The SO_2 total columns from the Brewer spectrophotometer MK II #037 located in Sodankylä (67.42° N, 26.59° E), Finland, are compared to the satellite retrievals. The SO_2 total columns are calculated from direct solar (DS) irradiances at the wavelengths of 306.3, 316.8 and 320.1 nm using the to-

tal ozone retrievals derived from the same instrument. The calibrations have been performed on regular basis. During the calibration, the extraterrestrial constant is determined using the Langley extrapolation method as described by Redondas (2007). Since the measurements at short wavelengths are affected by stray light effects, the DS measurements corresponding to high air mass values (after 14:20 UT) are not provided. No significant bias has been estimated during the calibration. The normal SO_2 values in Sodankylä are close to zero with an estimated detection limit of about 1 DU, similarly to the values reported by Rix et al. (2012) for Hohenpeissenberg. Georgoulias et al. (2009) found that the average SO_2 column values at most of the European Brewer sites are typically less than about 1 DU. Higher values of column SO_2 have been measured by Brewer instruments at sites affected by volcanic eruptions. For example, Fioletov et al. (1998) reported observations of column SO_2 amounts of more than 20 DU over Kagoshima (located close to a very active volcano, Sakurajima) as related to volcanic activity.

For this study, the atmospheric composition measurements were also available at four ground-level air quality monitoring stations located in northern Finland: Sammaltunturi (67.98° N, 24.12° E; 566 m), Kevo (69.76° N, 27.02° E; 107 m), Raja-Jooseppi (68.48° N, 28.30° E; 262 m), Oulanka (66.32° N, 29.42° E; 310 m). These remote rural-background monitoring sites have no significant SO_2 emission sources in the vicinity, but are occasionally affected by the industrial SO_2 emissions from the Kola Peninsula, Russia (about 10–15 kt in 2012 as reported in EMEP (European Monitoring and Evaluation Programme) database, http://www.ceip.at). The surface SO_2 concentrations were measured using online trace level gas analysers based on the ultraviolet fluorescence method (i.e. European reference method). Measurement height is 4–5 m. The concentrations are recorded at 1 min intervals and, in this study, the hourly average values are used.

3 Results and discussion

3.1 Timeline of Holuhraun eruption

On 16 August 2014 the first indications of increasing seismic activity close to the Bárðarbunga (64.60° N, −17.50° E) volcano were reported by the Icelandic Met Office (see http://en.vedur.is/earthquakes-and-volcanism/articles/nr/2947). On 31 August the eruption started in the Holuhraun fissure, located northeast from Bárðarbunga. It was a continuous effusive fissure eruption, without explosive activity.

Figure 1 shows the time evolution of the OMI TRL SO_2 maps over northern Europe during selected days after the volcanic eruption. The first enhanced SO_2 signal from satellite observations was detected over Iceland on 1 September (Fig. 1a). During the next days the SO_2 plume moved eastward toward Scandinavia (Fig. 1b). According to the satellite observations, the plume reached the first time northern Finland on 5 September (Fig. 1c). After that, high SO_2 total column values over large areas in northern Finland were observed on 10, 27 and 29 September (Fig. 1d–f). Figure S1 in the Supplement shows the respective OMPS TRL SO_2 maps. The SO_2 map for 11 September is included instead of 28 September, when no OMPS observations are available. Despite similar algorithm assumptions and overpass times, the difference between OMI and OMPS SO_2 total columns can be quite large, especially on the northern part of the Atlantic Ocean on 4 and 10 September. On the other hand, the spatial distributions of the SO_2 plume from the two instruments are similar.

The end of Holuhraun fissure eruption was declared on 28 February 2015. This study has been limited to September 2014, in order to avoid extremely challenging observing conditions for the satellite retrievals occurring during fall-winter. In fact, the sensitivity of the satellite measurements to atmospheric trace gases in the lower troposphere is significantly reduced for large solar and/or viewing angles or when the field of view is affected by the clouds. Furthermore, no observations are available during the deepest winter time because of the reduced sun light hours at high latitudes.

3.2 Comparison between satellite and ground-based SO_2 total columns

SO_2 total columns from Brewer observations in Sodankylä during 6 days on September 2014 are presented in Fig. 2 (black dots). Only selected days with a sufficient amount of Brewer DS measurements are considered. For comparison, SO_2 total columns from both OMI SP and OMPS overpasses over Sodankylä are shown in Fig. 2. OMI DB SO_2 data are also available but they are not included in Fig. 2 since several orbits were missing on the second half of September due to processing anomaly. For completeness, the OMI DB data (when available) are reported in Table 2, and their agreement with the ground-based observations will be discussed later in this section. The central pixels (5–55 for OMI and 4–33 for OMPS) are highlighted in Table 2. The satellite data sets include four SO_2 products with different a priori profile assumptions as described in Sect. 2. In OMI SP, the PBL data are processed using both the PCA (blue circles in Fig. 2) and the BRD (pink stars in Fig. 2) algorithms. OMI and OMPS DB data sets are processed using the BRD algorithm. An overview of the satellite overpasses over Sodankylä (during the same days shown in Fig. 2) are presented in Table 2, together with the Brewer SO_2 observations closest (within 30 min) to the satellite overpass time.

The best agreement between ground-based and satellite SO_2 total columns is generally found for the PBL product (blue circles and crosses, and pink stars in Fig. 2). In general, for high-latitudes cloud-free observation conditions, the PBL products are expected to underestimate SO_2, since much

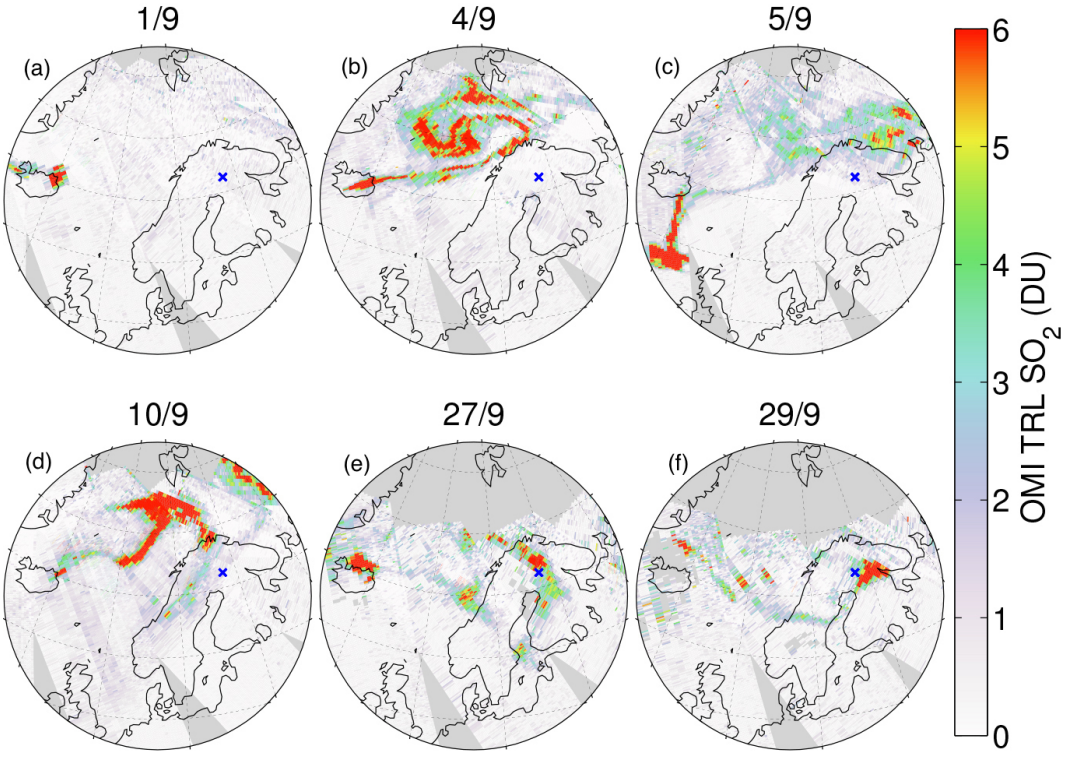

Figure 1. SO_2 total columns as seen from OMI SP TRL product during the Holuhraun fissure eruption for 6 days in September 2014. The dates (day/month) are indicated in the title of each panel. The blue crosses indicate the location of Sodankylä ground-based station.

smaller solar and viewing zenith angles are assumed in the retrievals (see Sect. 3.3). Furthermore, one must note that the satellite retrievals are expected to be lower than the Brewer values due to dilution, as the average SO_2 columns derived within the relatively large satellite pixel are compared to the local point measurements from ground-based observations. Overall, OMI retrievals are closer to the Brewer observations than OMPS. The results of the comparison are analysed day-by-day below.

5 September 2014 – The volcanic plume reaching Finland produces SO_2 total column values up to about 6 DU in Sodankylä as observed from the Brewer measurements. The best agreement with the SO_2 satellite products is achieved for OMI PBL data from the BRD algorithm. OMI SO_2 total column at 09:57 is 2.49 DU for the SP BRD data set and 2.85 DU for the DB data set, and the closest Brewer measurement is 3.7 DU. This overpass corresponds to favourable measuring conditions i.e. small OMI pixel (number 16), small distance between the pixel centre and the ground-based station (7.7 km), relatively small SZA (60.6°) and cloud fraction CF (0.21) smaller than 0.3. Overall the satellite retrieval gives smaller SO_2 vertical columns than the Brewer. Some of the possible reasons are discussed in Sect. 3.3.

6 September 2014 – Only OMI data are available because OMPS observations on Saturdays are dedicated to high resolution mode. One clear-sky overpass from OMI is available. Also in this case the satellite PBL product gives the best agreement with the corresponding Brewer retrieval. PCA and BRD algorithms give very similar results: SO_2 total column at 09:03 is 2.59 DU from BRD algorithm and 2.79 DU for PCA, while the closest Brewer measurement gives 4.4 DU. Also OMI PBL SO_2 total column value (3.86 DU) from direct broadcast is close to the ground-based observations. As on 5 September, this overpass corresponds to relatively good observation conditions (pixel number = 6, distance = 8 km, CF = 0.24 and SZA = 62.1°). As for 5 September satellite retrievals are smaller than Brewer measurements.

10 September 2014 – Two overpasses are available from both OMI and OMPS, but only one OMI overpass is under clear-sky conditions. Brewer data show again their best agreement with the PBL products. OMI SO_2 total column at 10:16 is 4.4 DU for PCA, 3.31 DU for BRD and 2.73 DU for the direct-broadcast BRD data set. The closest Brewer observation gives SO_2 total column value of 2.6 DU. OMPS data are very similar to OMI except for the PBL products.

27 September 2014 – From now on, the satellite overpasses correspond to SZA about 70° or larger. Only OMI overpasses are available, and only one is under clear-sky conditions. For this clear-sky overpass, OMI BRD PBL data are much closer than PCA to the ground-based observation. Also OMI TRL product is larger than PCA and closer to the ground-based observations. Very large SO_2 total column val-

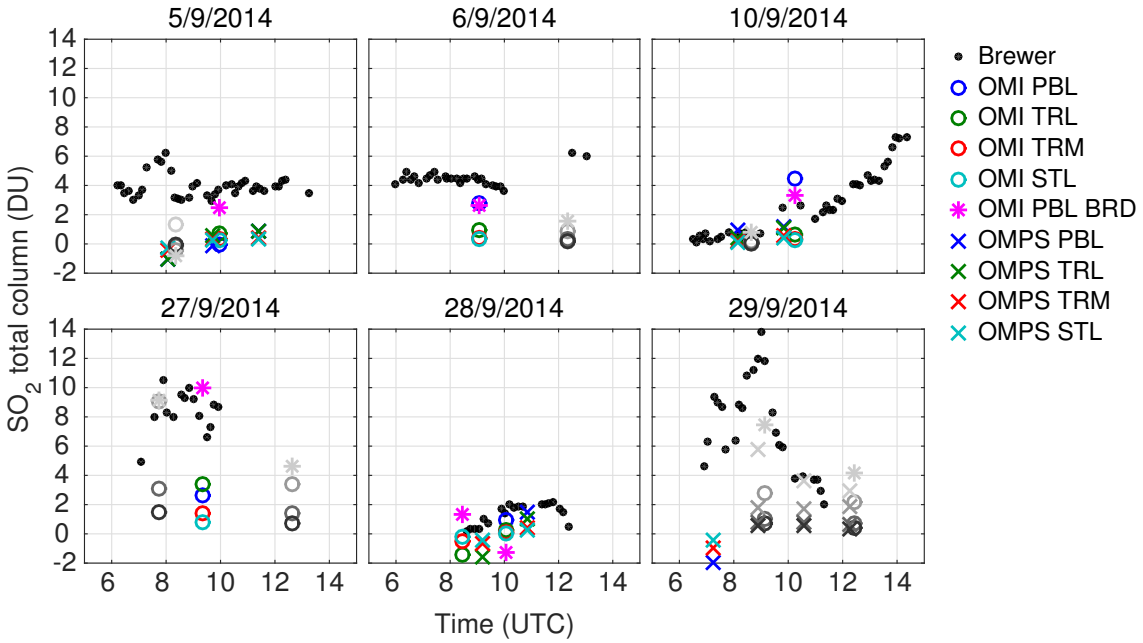

Figure 2. SO_2 vertical columns in Sodankylä, Finland during selected days of September 2014. Black dots refer to ground-based Brewer measurements, circles to OMI SP and crosses to OMPS observations. Different colours correspond to different satellite products sensitive to different altitude regions: PBL (blue), TRL (green), TRM (red) and STL (light blue). The pink stars refer to the PBL product processed using the BRD algorithm. PBL, TRL, TRM and STL satellite products for cloudy scenes (cloud fraction larger than 0.3) are shown in grey (from light to dark grey, respectively) and should be considered with caution.

ues (up to more than 10 DU) are observed by the Brewer. The largest satellite SO_2 total column (9.99 DU) is derived from the BRD algorithm from the standard product and it is very close to the Brewer values. OMI PBL product from direct broadcast gives a similar result (SO_2 total column is 9.50 DU).

28 September 2014 – The Brewer observations show SO_2 total column values up to about 2 DU, thus, much smaller than the previous days. Two clear-sky overpasses for both OMI and OMPS are available. Both OMI PBL PCA data and OMPS PBL are missing for the their first overpass of the day. For the second overpass, the PBL products are again very close to the ground-based observations, except for the OMI PBL product from the BRD algorithm which produces negative values. No OMI data from direct broadcast are available for this day.

29 September 2014 – The largest SO_2 total column (13.9 DU) from Brewer measurements in September is recorded. SZA values up to 74–75° are reached during this last day of comparison. Most of the overpasses are available under cloudy conditions and the only clear-sky overpass corresponds to a very large OMPS pixel (number 1) and large SZA (75.1°). No OMI PBL products from PCA algorithm are available. Despite these limitations, the satellite observations are able to follow the daily evolution of SO_2 total column shown by the ground-based measurements. Both OMI and OMPS PBL products (the lightest shade of grey in Fig. 2 – lower right panel) show larger values around 09:00 UTC and decreasing during the day.

The amount of satellite data included in the comparison can be increased considering all pixels within 60 km from Sodankylä. Figures S2 and S3 in the Supplement show the comparison between Brewer observations and this extended overpass data set for OMI and OMPS PBL products, respectively. In this case several overpasses correspond to almost the same time of the day. Because of the narrow structure of the SO_2 plume, this range of values corresponds to both in-plume and background pixels. For example, on 10 September, the large total column values from satellite retrievals agree with the Brewer observations obtained later in the afternoon, suggesting that the volcanic plume with higher SO_2 content (the blue-green narrow structure visible West from Sodankylä in Fig. 1d) reached Sodankylä after the overpass time. The largest difference between BRD and PCA algorithms can be observed on 27 September for SZA = 70°; because the PCA algorithm uses the entire spectrum in the SO_2 fitting to reduce interferences from instrumental or geophysical effects in general it was found PCA SO_2 results to be smaller than BRD, particularly for high latitudes. Furthermore, Sodankylä is often at the edge of the SO_2 plume, which is not optimal for comparisons. In Fig. S2 and S3 the data are separated according to the sky conditions and the pixels size, helping in visualising the results reported in Table 2. Satellite retrievals corresponding to large pixels are sometimes much

Table 2. Summary of the satellite overpasses at Sodankylä.

Date	Time	Data product[a]	CTP[b]	Distance[c]	CF[d]	SZA[e]	SO_2 total column (DU)[f]				Brewer DS[g]	
(09/14)	(UTC)			(km)			PBL[h]	TRL	TRM	STL	SO_2 (DU)	Time (UTC)
5	08:04	OMPS DB	3	58.2	0.29	64.2	−1.05	−1.04	−0.44	−0.30	6.2 ± 0.3	07:59
5	08:20	OMI SP	2	56.1	0.41	63.3	−0.84 / 1.30	−0.42	−0.11	−0.06	3.2 ± 0.4	08:18
5	08:20	OMI DB	2	56.1	0.41	63.3	−0.75	0.25	0.06	0.03	3.2 ± 0.4	08:18
5	**09:43**	**OMPS DB**	**12**	**23.2**	**0.21**	**60.6**	**−0.08**	**0.59**	**0.31**	**0.25**	**2.9 ± 0.5**	**09:39**
5	**09:57**	**OMI SP**	**16**	**7.7**	**0.22**	**60.6**	**2.49/−0.3**	**0.72**	**0.33**	**0.26**	**3.7 ± 0.3**	**09:56**
5	**09:57**	**OMI DB**	**16**	**7.7**	**0.21**	**60.6**	**2.85**	**1.20**	**0.51**	**0.38**	**3.7 ± 0.3**	**09:56**
5	**11:23**	**OMPS DB**	**31**	**33.2**	**0.25**	**61.9**	**0.88**	**0.91**	**0.41**	**0.31**	**3.9 ± 0.4**	**11:19**
6	**09:03**	**OMI SP**	**6**	**8.0**	**0.24**	**62.1**	**2.59 / 2.79**	**0.93**	**0.42**	**0.30**	**4.4 ± 0.3**	**09:02**
6	**09:03**	**OMI DB**	**6**	**8.0**	**0.24**	**62.1**	**3.86**	**1.66**	**0.68**	**0.47**	**4.4 ± 0.3**	**09:02**
6	12:19	OMI SP	58	13.3	0.44	64.6	1.53 / 0.25	0.86	0.30	0.18	6.2 ± 0.4	12:28
6	12:19	OMI DB	58	13.3	0.45	64.6	−0.09	0.89	0.27	0.17	6.2 ± 0.4	12:28
10	08:10	OMPS DB	3	19.7	0.25	65.4	0.93	0.45	0.19	0.13	0.7 ± 0.4	08:13
10	08:38	OMI SP	4	32.0	0.38	64.6	0.77 / 0.06	0.21	0.07	0.05	0.8 ± 0.2	08:27
10	08:38	OMI DB	4	32.0	0.39	64.6	0.94	0.70	0.23	0.15	0.8 ± 0.2	08:27
10	**09:49**	**OMPS DB**	**14**	**30.1**	**0.29**	**62.8**	**1.21**	**1.08**	**0.54**	**0.44**	**2.5 ± 0.5**	**09:48**
10	**10:16**	**OMI SP**	**22**	**8.1**	**0.15**	**62.4**	**3.31 / 4.44**	**0.65**	**0.36**	**0.27**	**2.6 ± 0.3**	**10:28**
10	**10:16**	**OMI DB**	**22**	**8.1**	**0.15**	**62.4**	**2.73**	**0.84**	**0.46**	**0.35**	**2.6 ± 0.3**	**10:28**
27	07:44	OMI SP	1	7.9	0.59	73.3	9.17 / –	9.07	3.06	1.50	8 ± 0.4	07:35
27	**09:21**	**OMI SP**	**8**	**17.2**	**0**	**69.4**	**9.99 / 2.66**	**3.42**	**1.37**	**0.81**	**6.6 ± 0.4**	**09:30**
27	**09:21**	**OMI DB**	**8**	**17.2**	**0**	**69.4**	**9.50**	**3.55**	**1.42**	**0.84**	**6.6 ± 0.4**	**09:30**
27	12:37	OMI SP	60	26.2	0.86	74.2	4.64 / –	3.41	1.39	0.70	–	–
28	08:26	OMI SP	3	19.1	0	71.6	1.36 / –	−1.40	−0.47	−0.23	0.2 ± 0.2	08:37
28	**09:12**	**OMPS DB**	**8**	**12.5**	**0.06**	**70.0**	**−2.94**	**−1.61**	**−0.66**	**−0.40**	**1.0 ± 0.3**	**09:14**
28	**10:03**	**OMI SP**	**18**	**4.0**	**0**	**69.4**	**−1.27 / 0.95**	**0.27**	**0.11**	**0.06**	**1.4 ± 0.2**	**10:02**
28	**10:52**	**OMPS DB**	**27**	**25.3**	**0.11**	**70.1**	**1.51**	**0.99**	**0.43**	**0.27**	**1.9 ± 0.2**	**10:40**
29	07:15	OMPS DB	1	8.5	0.04	75.3	−1.94	–	−1.00	−0.40	9.4 ± 1.3	07:17
29	**08:54**	**OMPS DB**	**6**	**11.9**	**0.41**	**70.7**	**5.76**	**1.81**	**0.77**	**0.55**	**12 ± 0.9**	**08:52**
29	**09:09**	**OMI SP**	**7**	**24.9**	**0.73**	**70.5**	**7.44 / –**	**2.81**	**1.06**	**0.73**	**11.8 ± 0.8**	**09:08**
29	**10:34**	**OMPS DB**	**23**	**6.4**	**0.31**	**70.1**	**3.66**	**1.75**	**−0.81**	**0.58**	**3.9 ± 0.8**	**10:31**
29	12:15	OMPS DB	36	40.8	0.55	74.2	2.91	1.84	0.61	0.32	–	–
29	12:25	OMI SP	59	28.3	0.71	74.2	4.20 / –	2.14	0.76	0.39	–	–

[a] Satellite data products. The options are the following: OMI SP (standard product); OMI DB (Direct Broadcast) and OMPS DB.
[b] Cross track position (CTP). Ranging from 1 to 60 for OMI and from 1 to 36 for OMPS. The central pixels (nadir) are smaller than those at the edges of the swath and they are highlighted in bold.
[c] Distance between the centre of the satellite pixel and Sodankyä.
[d] Satellite-derived cloud fraction (CF).
[e] Satellite-derived solar zenith angle (SZA).
[f] Satellite SO_2 total column optimised for different altitude regions: planetary boundary layer (PBL), lower troposphere (TRL), mid-troposphere (TRM) and lower stratosphere (STL).
[g] SO_2 total column from Brewer spectrophotometer direct sun (DS) measurements. The closest observations (within 30 min) to the satellite overpass time are taken into account.
[h] OMI SP PBL product is processed using both band residual difference and principal component analysis algorithms (BRD / PCA).

smaller than Brewer observations (see, e.g. light blue markers on 5 and 29 September in Fig. S3, where negative values are reported). Under cloudy conditions, the satellite retrievals are expected to underestimate the SO_2 columns, since part of the column is below the cloud. This behaviour it is not clearly visible from Figs. S2 and S3, because several factors are affecting the analysis.

3.3 Analysis of the uncertainties

In order to to get an idea about the precision (or noise) of the satellite data at northern high latitudes, STDs for different products are derived from the box (10° E, 30° E) × (60° N, 70° N) for a presumably SO_2-free day (1 September 2014). For TRL, TRM and STL products, the obtained standard deviation values are very similar to those reported in the README file (see Sect. 2). For the PBL products, STDs of about 1.6 DU, 0.8 DU and 0.5 DU are obtained for OMI BRD, OMI PCA and OMPS BRD products, respectively. On 3 October 2014, with solar zenith angles about 70° or higher, the STD values are about 2.7 and 2.1 DU for OMI and OMPS PBL BRD products and about 1.1 DU for OMI PCA PBL data product. In addition, TRL STDs grow up to about 1.2 DU. This confirms that the quality of the satellite retrieval is lower for high solar zenith angles. The overpasses shown in Fig. 2 are sometimes close or below the detection limit (defined as twice the precision), especially during the last days of comparison. Assuming that the PBL products better represent the actual SO_2 profile distribution, the differences between satellite and ground-based observations are mostly within these uncertainties.

One of the main source of error in the BRD product is due to the fact that the vertical column density is obtained dividing the slant column density by a constant AMF of 0.36, which is derived for SZA = 30° and VZA = 0°. The same settings are used in the PCA algorithm. The radiative transfer calculation shows (Fig. S4 in the Supplement) that the AMF decreases by about 30 % from 30° to 65° SZA, leading to an underestimation of the SO_2 vertical column. There is also less pronounced dependence on the VZA. The operational vertical column can be corrected by multiplying by the ratio between the assumed AMF (0.36) and the AMF calculated

for larger values of SZA and VZA (Krotkov et al., 2008). For example, when correcting the operational retrievals for SZA = 60° (as for example on 5 September) with AMF about 0.3, the resulting SO_2 vertical column is 20 % larger than the operational value.

The AMF also depends on the slant column ozone (SCO). To the first approximation the dependence can be approximated as a linear regression with SCO amount as described in Fig. 4 in Krotkov et al. (2008). For SCO values larger than 1500 DU (high ozone and/or high solar zenith and viewing angles, as at high latitudes) the AMF decreases by more than 30 %.

Figure S5 in the Supplement includes the comparison between Brewer SO_2 columns and OMI and OMPS PBL products corrected for a range of possible AMF values (0.2–0.4, considering SZA = 60°–75°, VZA = 0°–45°, SCO = 800–1600 DU). The resulting SO_2 columns range from 80 % larger and 10 % smaller than the operational values. Because satellite retrievals often underestimate the ground-based observations, the results of the comparison are generally improved using a smaller AMF values. In some cases (e.g. OMI BRD product on 27 September), correcting for a smaller value of AMF, does not improve the results of the comparison. Because the AMF correction is a multiplicative factor, the variability of the SO_2 column value depends on the original value. Thus, SO_2 column values close to zero or negative will have very small variability or will become more negative when changing the AMF value. It must be also pointed out that the "error bars" presented in Fig. S5 include only the variability due to different AMF values, but not other sources of uncertainty.

On the other hand, the LF algorithm accounts for the actual observation conditions and has no inherent bias under high solar/viewing zenith angles.

Another source of error in the satellite retrievals is due to the difference between the assumed profiles and the actual SO_2 layer height. The averaging kernels represent the height-dependent sensitivity of the satellite observations to changes in the SO_2 amount. Considering for example the LF averaging kernels (Fig. S6 in the Supplement and Yang et al., 2007), the retrieved SO_2 column can be further adjusted with the actual layer height. For instance, for an SO_2 layer centred at 1 km, the LF TRL retrieval underestimates the column amount: the actual SO_2 column is twice as large as TRL columns for a cloud-free scene. Also, the averaging kernels show similar dependence on altitude for various viewing and solar zenith angles (different line colours in Fig. S6), especially for altitudes below the assumed CMA. Thus, no significant changes are expected for high latitude observations. The PBL retrievals are characterised by a similar altitude dependence as for the LF algorithm.

Overall, the SO_2 retrieval at high latitudes is challenging due to low earthshine radiance received from the satellite; thus large impacts of instrumental effects (such as stray lights and other spectral artifacts) are expected on the retrieval results. This leads to biases which can exceed those from measurement noises and retrieval errors due to algorithmic assumptions described above.

3.4 Effect of volcanic SO_2 emission on the surface-level concentration

Since the volcanic SO_2 plume was located at low altitudes, elevated concentrations of SO_2 were detected also at the surface. Figure 3 (right panel) shows the time evolution of the SO_2 concentrations observed during September 2014 at four air quality stations in northern Finland: Sammaltunturi, Kevo, Raja-Jooseppi and Oulanka. The locations of these sites are shown as triangles in Fig. 3 (left panel). Elevated SO_2 concentration values were measured starting on 5 September 2014, when also the SO_2 plume was observed over northern Finland for the first time after the volcanic eruption (Fig. 1c). The highest hourly mean (about 180 $\mu g\,m^{-3}$) was found at Sammaltunturi during the night between 7 and 8 September 2014. The largest daytime peak at Sammaltunturi was observed on 10 September. During the same day concentration peaks were observed also at Raja-Jooseppi and Kevo stations. For comparison, the map of OMI PBL PCA product on 10 September is shown in Fig. 3 (left panel): the three northernmost stations (Sammaltunturi, Kevo and Raja-Jooseppi) were inside the SO_2 plume. This corresponds to the SO_2 concentration peaks observed in Fig. 3 (right panel) on 10 September. On the other hand, Oulanka was outside the plume during the same day and large SO_2 concentrations were only observed the morning after, 11 September 2014, because the plume was transported eastward (as seen in Fig. S1). The SO_2 concentration peak in Kevo was smaller than in the other sites probably due to the lower altitude of the station.

Large SO_2 concentrations were measured during 13–19 September 2014 (up to about 50 $\mu g\,m^{-3}$ on 15 September), corresponding to SO_2 total column values up to about 1.5 DU measured from Brewer during the same period (not shown here). Because only sparse Brewer DS measurements are available during this period, these data are not included in the comparison shown in Fig. 2. Elevated SO_2 concentrations (up to about 50 $\mu g\,m^{-3}$) were observed also on 27 and 29 September, when also the Brewer and the satellite measurements showed high SO_2 total column values. These concentrations were not as elevated as in the first half of September. This suggests that the SO_2 plume was located at higher altitudes during these 2 last days, thus only partially affecting the SO_2 concentration levels at the surface.

Despite satellite vertical columns and ground-based surface concentrations are not quantitatively comparable, the observed spatiotemporal link between high SO_2 concentration values at surface and large total columns from satellite adds confidence in using satellite-based observations for volcanic emission monitoring during such kind of events, with the SO_2 plume located at quite low altitudes. In particular,

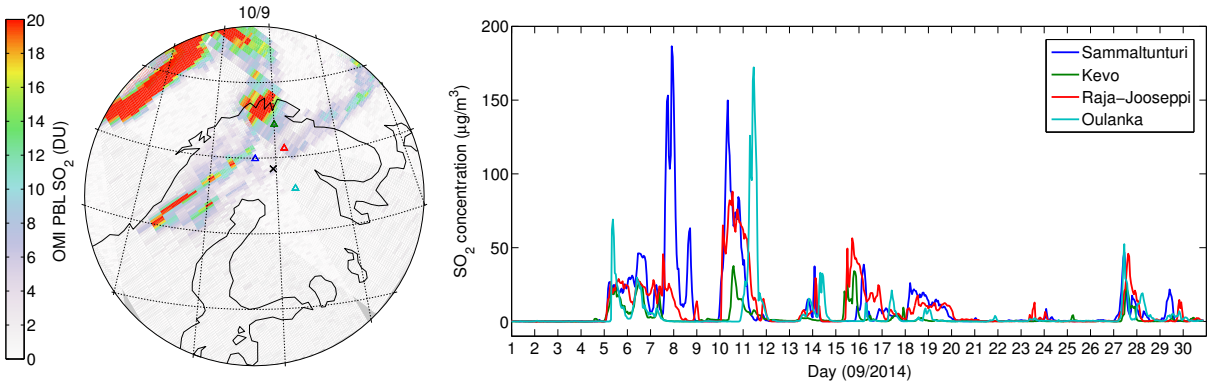

Figure 3. Left panel: OMI SP PBL (PCA algorithm) during 10 September 2014. The black cross indicates the location of Sodankylä. The triangles indicate the location of the air quality stations: Sammaltunturi (blue), Kevo (green), Raja-Jooseppi (red), Oulanka (light blue). Right panel: Time series of the SO_2 concentration in the northern Finland air quality stations in September 2014.

in this case the satellite instruments showed their capability to detect the position of the volcanic plume as compared to independent ground-based observations.

4 Summary and remarks

The comparison of satellite SO_2 retrievals derived from the OMI and OMPS instruments with ground-based observations during the Icelandic Holuhraun fissure eruption in September 2014 is presented in this paper. The satellite observations were compared against ground-based Brewer measurements made in Sodankylä, Finland, which is located more than 2000 km from the emission source. On 29 September 2014, the Brewer measured the SO_2 total column record value (13.9 DU) for 2014. This is the second largest value measured in Sodankylä, after the Kasatochi volcanic eruption in 2008 (17.2 DU).

The best agreement with the Brewer data was usually achieved with the satellite data products that assume a priori profile with SO_2 predominantly in the planetary boundary layer, i.e. the lowest levels of the atmosphere. This is reasonable since the SO_2 emissions in Iceland were emitted at tropospheric altitudes. In addition, exceptionally high SO_2 surface concentrations (up to about 180 $\mu g\,m^{-3}$) were observed in northern Finland, where the typical background SO_2 concentrations are close to zero. The air quality monitoring site located at the highest altitude, Sammaltunturi, was the most affected; hourly SO_2 concentration exceeded 100 $\mu g\,m^{-3}$ 15 times. Record high concentrations were also detected at Oulanka, where the highest hourly, daily and monthly averages in the past 10 years were recorded. The SO_2 concentration peaks in the time series correspond to enhanced SO_2 signals in the satellite data observed on the same days. This supports the hypothesis that the volcanic plume was located very close to the surface. These results show also that the satellite retrieval algorithms can detect, qualitatively, the geographical location of the SO_2 plume, as compared to the ground-based stations.

The comparison between satellite and Brewer SO_2 total columns showed the best agreement during the first half of September. During this first period, the BRD and the new PCA algorithms give very similar results for the OMI PBL product. Also the OMI DB products were available until 27 September. The direct-broadcast and standard products showed very similar results. The discrepancy between these products (both derived using the BRD algorithm) is related to the different residual correction methods.

In the latter comparison period, the agreement with satellite products was weaker and the best agreement was found with PBL and TRL data products. The weaker agreement can be related to the less favourable satellite retrieval conditions, e.g. the large solar zenith angles (close or above 70°) and the frequent cloudy conditions. Less OMI PBL data from PCA algorithm were available, because the retrievals with slant column O_3 over 1500 DU (corresponding to high O_3 and large solar and viewing angles) are not included in the data set. Also, the different OMI PBL products (PCA and BRD) gave less similar results than at the beginning of September. Despite these limitations, the satellite observations were still able to follow the daily evolution of the Brewer SO_2 total column values.

There are not many validation studies including satellite SO_2 data and even less at high latitudes. This is the first work in which PBL products are used to analyse volcanic emissions, because the SO_2 plume was located at very low altitudes. Because the solar and viewing zenith angles assumed in the satellite retrieval refer to lower-latitude regions, the satellite data for PBL are expected to underestimate SO_2 at high latitudes. Furthermore, the knowledge of the SO_2 vertical profile is critical to evaluate how the satellite retrievals compare to the actual SO_2 column. This study highlights the need for improved retrievals at high latitudes and provides useful information about satellite SO_2 data qual-

ity during a volcanic eruption episode with several peculiarities: the SO_2 plume was found close to the surface and strongly affected the air quality levels in northern Finland; the ground-based station Sodankylä is located at high latitudes (above 67° N), where the satellite retrievals are particularly challenging because of high solar zenith angles and frequent cloudy scenes; the absolute SO_2 values are much higher than the background, reaching up to 9 DU in this study. Also, this is the first time when direct-broadcast SO_2 satellite data (from both OMI and OMPS instruments) are compared against ground-based observations.

The end of Holuhraun fissure eruption was declared at the end of February 2015, meaning that the eruption continued during the northern hemispheric winter. Monitoring SO_2 during winter using UV-VIS instruments like OMI and OMPS becomes more difficult because of the reduced length of the day and increasing solar zenith angles. This can be already seen, e.g. in Fig. 1: the observable area is quickly reduced moving from the beginning to the end of September. For this reason, this study was limited to the month of September only. In addition to instruments like OMI and OMPS, SO_2 can be measured using satellite instruments like IASI (Infrared Atmospheric Sounding Interferometer, e.g. Clarisse et al., 2008) and AIRS (Atmospheric Infrared Sounder, e.g. Carn et al., 2005), which use the IR channels. However, they are less sensitive than the UV-VIS instruments to the tropospheric SO_2 signal.

The Supplement related to this article is available online at doi:10.5194/amt-8-2279-2015-supplement.

Acknowledgements. The FMI work is supported by the Academy of Finland (INQUIRE project), by TEKES (SPARK project) and by ESA (ILMA Living Planet fellowship). The standard product data are distributed through the NASA's MIRADOR website (http://mirador.gsfc.nasa.gov), while the direct-broadcast data are obtained from FMI's SAMPO service (http://sampo.fmi.fi).

Edited by: S. Beirle

References

Brenot, H., Theys, N., Clarisse, L., van Geffen, J., van Gent, J., Van Roozendael, M., van der A, R., Hurtmans, D., Coheur, P.-F., Clerbaux, C., Valks, P., Hedelt, P., Prata, F., Rasson, O., Sievers, K., and Zehner, C.: Support to Aviation Control Service (SACS): an online service for near-real-time satellite monitoring of volcanic plumes, Nat. Hazards Earth Syst. Sci., 14, 1099–1123, doi:10.5194/nhess-14-1099-2014, 2014.

Carn, S. A. and Lopez, T. M.: Opportunistic validation of sulfur dioxide in the Sarychev Peak volcanic eruption cloud, Atmos. Meas. Tech., 4, 1705–1712, doi:10.5194/amt-4-1705-2011, 2011.

Carn, S., Strow, L., de Souza-Machado, S., Edmonds, Y., and Hannon, S.: Quantifying tropospheric volcanic emissions with AIRS: the 2002 eruption of Mt. Etna (Italy), Geophys. Res. Lett., 32, L02301, doi:10.1029/2004GL021034, 2005.

Carn, S. A., Krueger, A. J., Krotkov, N. A., Yang, K., and Evans, K.: Tracking volcanic sulfur dioxide clouds for aviation hazard mitigation, Nat. Hazards, 51, 325–343, doi:10.1007/s11069-008-9228-4, 2008.

Carn, S. A., Yang, K., Prata, A. J., and Krotkov, N. A.: Extending the long-term record of volcanic SO_2 emissions with the Ozone Mapping and Profiler Suite nadir mapper, Geophys. Res. Lett., 42, 925–932, doi:10.1002/2014GL062437, 2015.

Charlson, R. J., Langner, J., and Rodhe, H.: Sulphate aerosol and climate, Nature, 348, 6296, doi:10.1038/348022a0, 1990.

Clarisse, L., Coheur, P. F., Prata, A. J., Hurtmans, D., Razavi, A., Phulpin, T., Hadji-Lazaro, J., and Clerbaux, C.: Tracking and quantifying volcanic SO_2 with IASI, the September 2007 eruption at Jebel at Tair, Atmos. Chem. Phys., 8, 7723–7734, doi:10.5194/acp-8-7723-2008, 2008.

Fioletov, V. E., Griffioen, E., Kerr, J. B., Wardle, D. I., and Uchino, O.: Influence of volcanic sulfur dioxide on spectral UV irradiance as measured by Brewer spectrophotometers, Geophys. Res. Lett., 25, 1665–1668, doi:10.1029/98GL51305, 1998.

Fioletov, V. E., McLinden, C. A., Krotkov, N., Moran, M. D., and Yang, K.: Estimation of SO_2 emissions using OMI retrievals, Geophys. Res. Lett., 38, L21811, doi:10.1029/2011GL049402, 2011.

Fioletov, V. E., McLinden, C. A., Krotkov, N., Yang, K., Loyola, D. G., Valks, P., Theys, N., Van Roozendael, M., Nowlan, C. R., Chance, K., Liu, X., Lee, C., and Martin, R. V.: Application of OMI, SCIAMACHY, and GOME-2 satellite SO_2 retrievals for detection of large emission sources, J. Geophys. Res., 118, 1–20, doi:10.1002/jgrd.50826, 2013.

Flynn, L. E., Seftor, C. J., Larsen, J. C., and Xu, P.: The ozone mapping and profiler suite, in: Earth Science Satellite Remote Sensing, Science and Instruments, 1, edited by: Qu, J. J., Gao, W., Kafatos, M., Murphy, R. E., and Salomonson, V. V., Springer, Berlin, Heidelberg, Germany, 279–296, 2006.

Georgoulias, A. K., Balis, D., Koukouli, M. E., Meleti, C., Bais, A., and Zerefos, C.: A study of the total atmospheric sulfur dioxide load using ground-based measurements and the satellite derived sulfur dioxide index, Atmos. Environ., 43, 1693–1701, doi:10.1016/j.atmosenv.2008.12.012, 2009.

Gurevich, G. S. and Krueger, A. J.: Optimization of TOMS wavelength channels for ozone and sulfur dioxide retrievals, Geophys. Res. Lett., 24, 2187–2190, doi:10.1029/97GL02098, 1997.

Hassinen, S., Tamminen, J., Tanskanen, A., Koskela, T., Karhu, J. M., Lakkala, K., Mälkki, A., Leppelmeier, G., Veefkind, P., Krotkov, N., and Aulamo, O.: Description and validation of the OMI very fast delivery products, J. Geophys. Res., 113, D16S35, doi:10.1029/2007JD008784, 2008.

Hofmann, D. J. and Solomon, S.: Ozone destruction through heterogeneous chemistry following the eruption of El Chichón, J. Geophys. Res., 94, 5029–5041, doi:10.1029/JD094iD04p05029, 1989.

Krotkov, N. A., Carn, S. A., Krueger, A. J., Bhartia, P. K., and Yang, K.: Band residual difference algorithm for retrieval of SO_2 from the aura ozone monitoring instru-

ment (OMI), IEEE T. Geosci. Remote, 44, 1259–1266, doi:10.1109/TGRS.2005.861932, 2006.

Krotkov, N. A., McClure, B., Dickerson, R. R., Carn, S. A., Li, C., Bhartia, P. K., Yang, K., Krueger, A. J., Li, Z., Levelt, P. F., Chen, H., Wang, P., and Lu, D.: Validation of SO_2 retrievals from the ozone monitoring instrument (OMI) over NE China, J. Geophys. Res., 113, D16S40, doi:10.1029/2007JD008818, 2008.

Krueger, A. J.: Sighting of El Chichón sulfur dioxide clouds with the Nimbus 7 Total Ozone Mapping Spectrometer, Science, 220, 1377, doi:10.1126/science.220.4604.1377, 1983.

Krueger, A. J., Krotkov, N. A., and Carn, S. A.: El Chichon: The genesis of volcanic sulfur dioxide monitoring from space, J. Volcanol. Geoth. Res., 175, 408–414, doi:10.1016/j.jvolgeores.2008.02.026, 2008.

Leppelmeier, G., Aulamo, O., Hassinen, S., Mälkki, A., Riihisaari, T., Tajakka, R., Tamminen, J., and Tanskanen, A.: OMI very fast delivery and the Sodankylä satellite data centre, IEEE T. Geosci. Remote, 44, 1283–1287, doi:10.1109/TGRS.2005.863718, 2006.

Levelt, P. F., van den Oord, G. H. J., Dobber, M. R., Mälkki, A., Visser, H., de Vries, J., Stammes, P., Lundell, J., and Saari, H.: The ozone monitoring instrument, IEEE T. Geosci. Remote, 44, 1093–1101, doi:10.1109/TGRS.2006.872333, 2006.

Li, C., Joiner, J., Krotkov, N. A., and Bhartia, P. K.: A fast and sensitive new satellite SO_2 retrieval algorithm based on principal component analysis: Application to the ozone monitoring instrument, Geophys. Res. Lett., 40, 6314–6318, doi:10.1002/2013GL058134, 2013.

McLinden, C. A., Fioletov, V., Boersma, K. F., Krotkov, N., Sioris, C. E., Veefkind, J. P., and Yang, K.: Air quality over the Canadian oil sands: a first assessment using satellite observations, Geophys. Res. Lett., 39, L04804, doi:10.1029/2011GL050273, 2012.

Redondas, A.: Ozone absolute Langley calibration, edited by: McElroy, C. T. and Hare, E. W., The Tenth Biennial WMO Consultation on Brewer Ozone and UV Spectrophotometer Operation, Calibration and Data Reporting, GAW Report No.176 (WMO TD No. 1420), Northwich, United Kingdom, 4–8 June 2007, edited by: McElroy, C. T. and Hare, E. W., 12–14, 2007.

Rix, M., Valks, P., Hao, N., van Geffen, J., Clerbaux, C., Clarisse, L., Coheur, P.-F., Loyola, D., Erbertseder, T., Zimmer, W., and Emmadi, S.: Satellite monitoring of volcanic sulfur dioxide emissions for early warning of volcanic hazards, IEEE J. Sel. Top. Appl., 2, 196–206, doi:10.1109/JSTARS.2009.2031120, 2009.

Rix, M., Valks, P., Hao, N., Loyola, D., Schlager, H., Huntrieser, H., Flemming, J., Koehler, U., Schumann, U., and Inness, A.: Volcanic SO_2, BrO and plume height estimations using GOME-2 satellite measurements during the eruption of Eyjafjallajökull in May 2010, J. Geophys. Res., 117, D00U19, doi:10.1029/2011JD016718, 2012.

Spinei, E., Carn, S. A., Krotkov, N. A., Mount, G. H., Yang, K., and Krueger, A. J.: Validation of ozone monitoring instrument SO_2 measurements in the Okmok volcanic cloud over Pullman, WA in July 2008, J. Geophys. Res., 115, D00L08, doi:10.1029/2009JD013492, 2010.

Yang, K., Krotkov, N. A., Krueger, A. J., Carn, S. A., Bhartia, P. K., and Levelt, P. F.: Retrieval of large volcanic SO_2 columns from the aura ozone monitoring instrument: comparison and limitations, J. Geophys. Res., 112, D24S43, doi:10.1029/2007JD008825, 2007.

Yang, K., Dickerson, R. R., Carn, S. A., Ge, C., and Wang, J.: First observations of SO_2 from the satellite Suomi NPP OMPS: Widespread air pollution events over China, Geophys. Res. Lett., 40, 4957–4962, doi:10.1002/grl.50952, 2013.